
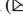




Probabilistic Assessment of RC Piers Considering Vertical Seismic Excitation Based on Damage Indices

S. Mahboubi¹ , M. R. Shiravand¹ , G. Shid¹, and M. Kioumarsi²

¹ Faculty of Civil, Water and Environmental Engineering, Shahid Beheshti University, Tehran, Iran

{Sh_Mahboubi, M_Shiravand}@sbu.ac.ir

² Department of Civil Engineering and Energy Technology, OsloMet-Oslo Metropolitan University, Oslo, Norway

Abstract. Bridges play a vital role in highway transportation systems and damage to bridges may cause impaired emergency response and economic loss and interrupt the functionality of the systems. Damage to bridge during the last earthquakes shows that considering the effects of the vertical component of earthquakes in seismic damage assessment of reinforced concrete (RC) piers is of great importance. This paper aims to assess the probability of damage to RC columns under the simultaneous effect of three earthquake components. For this purpose, two damage indices including strain and curvature ductility have been used and the fragility curves of RC columns have been developed with Probabilistic Seismic Demand Models (PSDM) under a series of ground motion records. Moreover, the variation of axial force, bending moment, and shear force have been investigated. The results show that considering the vertical excitation may increase the probability of different damage states of RC columns, particularly in higher damage states.

Keywords: Bridge · PSDM · Damage Indices · RC Columns · Vertical Component

1 Introduction

All types of bridges, including integral highway bridges, may be damaged by vertical acceleration in seismically potential regions. Commonly, vertical motion of an earthquake is not explicitly considered in the design of ordinary highway bridges [1], and consequently, the effect of vertical motion is generally neglected. Vertical components of an earthquake have significantly lower energy contents than horizontal components. Thus, they are insignificant in terms of damage potential due to their low energy contents [2, 3]. Although current seismic design requirements do not attempt to account for the vertical motion effect, it can be crudely included in design codes by increasing or decreasing the dead load actions in load combination equations. According to the Caltrans Seismic Design Criteria [1], an equivalent static load should be applied to the

superstructure of ordinary standard bridges when the peak ground acceleration of the site is at least 0.6 g. In order to assess the effects of vertical excitation, about 25% of the dead load applies to the upward and downward of the superstructure uniformly. In contrast, this approach is clearly not quite accurate when it comes to variables like seismic conditions of the bridge region, magnitude and epicentre of a potential earthquake, and vertical-to-horizontal acceleration ratio [4].

In general, reinforced concrete buildings suffered significant structural damage during the Northridge 1994 Earthquake, and many instances of intermediate storey damage or even collapse were observed because of different reasons, such as abrupt changes in stiffness and strength in elevation or the lack of a capacity design approach in higher storeys [5–7]. Moreover, the substructure mass shows higher impacts on bridge performance when the acceleration is applied in the vertical direction and leading to inertia forces. But this effect can be ignored in bridges with short piers or bridges with hollow section piers [8].

According to previous investigations, Saadeghvaziri and Foutch [9, 10] reported that the variable forces induced by the vertical motion on the abutments are not included in seismic design guidelines. They used a finite element code capable of modeling the inelastic behavior of RC columns under combined horizontal and vertical deformations. In their study, they showed that varying axial forces caused fluctuations in column shear capacities and reduced their ability to dissipate energy.

According to Broderick and Elnashai [11] and Papazoglou and Elnashai [12], significant fluctuations in axial forces in vertical elements reduce column shear capacity because of the strong vertical ground motion. A parametric study of the effects of vertical acceleration on bridges was conducted by Yu et al. [13], as well as Yu et al. [14]. Three overpass bridges were analysed using three-dimensional (3D) linear models to determine the effects of the vertical component of excitation on the piers, foundations, bearings, and hinges. In Yu's study, vertical motion increased the axial force and longitudinal moment of the pier by 20% and 7%, respectively. Button et al. [15] investigated the combined effects of horizontal and vertical motion on ground motion. A total of six bridges were evaluated under this situation, representing events with magnitudes 6.5 and 7.5. Most of their studies were limited to linear response spectrums and linear dynamic analyses. It was concluded from the results that vertical ground motion significantly affected the axial forces, especially at the bridge sites with fault distances less than 10–20 km. Other studies have been conducted on this object, and most confirm that vertical loads cause the final failure collapse and have a significant change on the axial forces of bridge piers [16, 17].

In this study, the effects of the vertical component of earthquakes on RC piers of an Integral Bridge (IB) have been investigated. For this purpose, nonlinear responses of a two-span continuous deck RC bridge are evaluated through finite element (FE) modelling. The Nonlinear Time History Analysis (NLTHA) is performed with a wide range of ground motion parameters to consider the various ratio of vertical peak acceleration to horizontal peak acceleration (V/H). Probabilistic Seismic Demand Models (PSDM) are generated from analyses with and without considering the vertical component of motion. Fragility curves are developed with two different damage indices, including strain and curvature ductility. The curvature damage limits are based on Desroches and

Ramanathan's report [18], and the strain-based damage limits are defined by the authors. The results are compared to evaluate the effects of vertical ground motion.

2 Description of Model

The selected bridge for the NLTHA is a two-span continuous concrete deck bridge with an integral connection between the superstructure and substructure. The length of the spans is 20 m and the height of the RC columns is 8 m, which contain longitudinal reinforcement and transverse hook stirrups. The columns are assumed to be fixed at the soil foundation [19]. The cross-sectional diameter of all piers is 1.2 m. Details of the modeling and dimensions of the bridge are presented in Figs. 1 and 2.

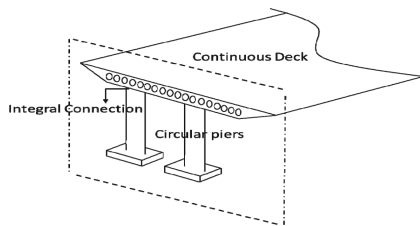


Fig. 1. Cross-section of a bridge.

2.1 Finite Element Modeling

A Three-dimensional (3D) fiber-based model of the bridge is developed in the Open System for Earthquake Engineering Simulation (OPENSEES) [20]. A general layout and nodal scheme of the model are illustrated in Figs. 2 and 3. The deck is assumed to remain elastic during seismic loading and be undamaged under earthquakes. Hence, the deck is modeled with equivalent linear-elastic beam-column elements. The Non-linearBeamColumn element is used for modeling the nonlinear behavior and plasticity distribution along the element length. The cross-section of the piers is discretized into fibers of confined and unconfined concrete and reinforcing steel bars as shown in Fig. 3. Fiber sections can simulate the interaction between axial and flexural forces, which is an important effect under vertical loads. The connection between the superstructure and substructure is modeled with rigid elements. The confined and unconfined concrete behavior is modeled using the concrete07 material of OPENSEES, which considers the concrete tensile strength. The unconfined compressive strength of concrete material is equal to 33.8 MPa and the compressive strength of confined concrete is defined with respect to the equations developed by Mander et al. [21]. The steel02 model [22] is used for modeling reinforcing bars in the bridge piers with a yield strength of 460 MPa and an elastic modulus of 200 GPa. The stress-strain behavior of materials is shown in Fig. 3(b).

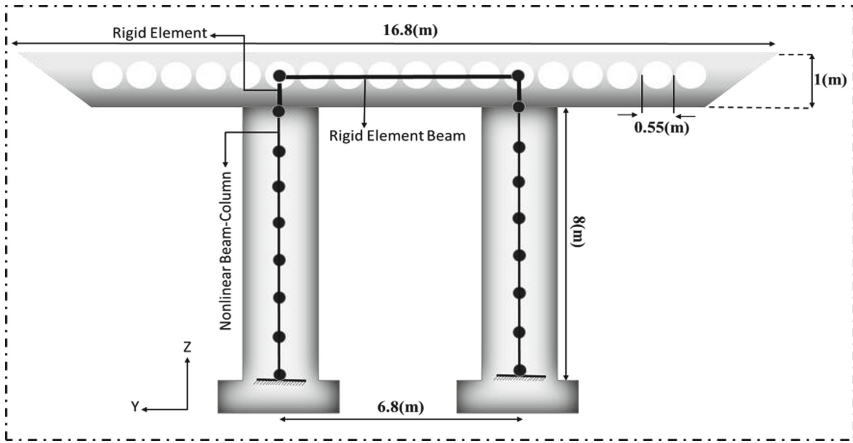
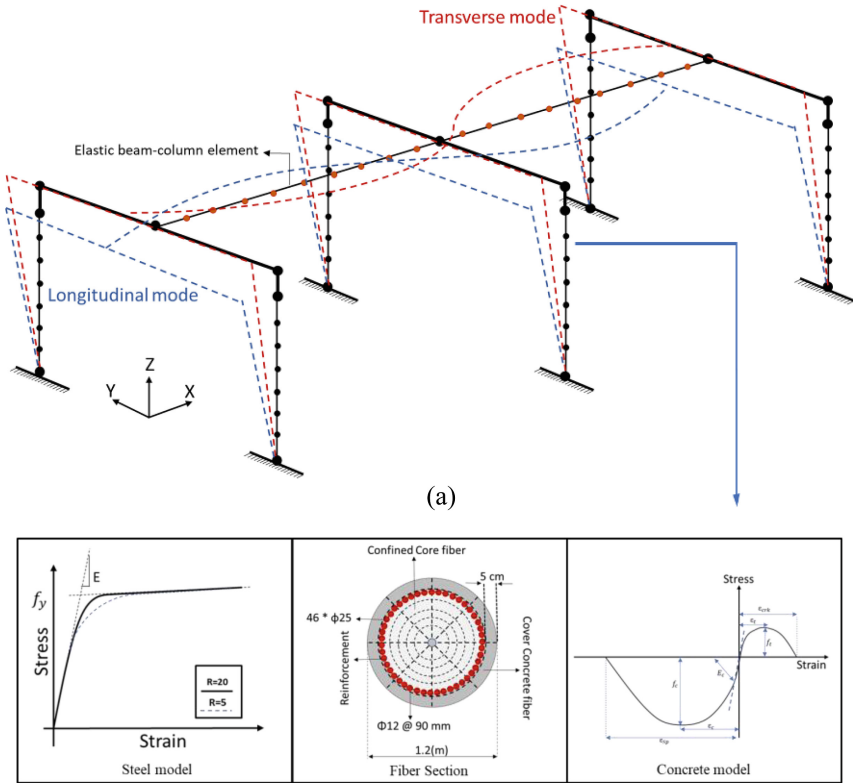


Fig. 2. Detailed elements.



(b)

Fig. 3. (a) Nodal scheme and two first modes of vibration contain 1. Longitudinal mode, and 2. Transverse mode. (b) Fiber section and materials stress-strain diagrams.

3 Probabilistic Seismic Demand Models and Damage Limit States

In order to perform a probabilistic seismic analysis of structures, seismic demand models must be constructed. Therefore, a Probabilistic Seismic Demand Analysis (PSDA) was conducted by NLTHA of the bridge with 100 earthquake ground motions. NLTHA is typical of the cloud approach [23]. Cloud analysis is a numerical procedure in which a structure is subjected to (unscaled) ground motions and the results are analyzed numerically. Figure 4 shows a typical PSDM on a logarithmic scale.

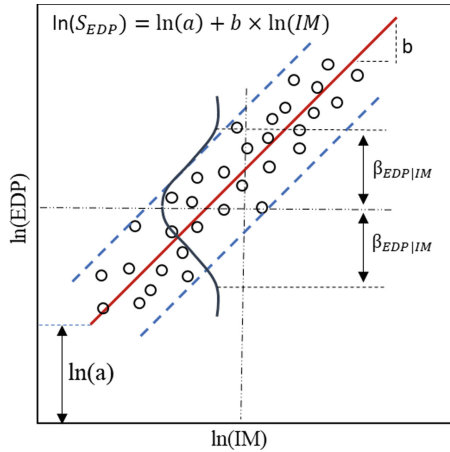


Fig. 4. Typical PSDM.

The fragility function is a relationship between the peak Engineering Demand Parameter (EDP) and the Intensity Measure (IM). In this study, strain and curvature ductility are selected as EDPs and Peak Ground Acceleration (PGA) [24] is selected as IM.

Cornell et al. [25] formulated this conditional relationship which is called PSDM. Cloud analysis results are used to develop this model. In this equation, the EDP data are assumed to have a lognormal distribution when conditioned on the IM.

$$P[D \geq d | IM] = 1 - \Phi\left(\frac{\ln(d) - \ln(S_D)}{\beta_{D|IM}}\right) \tag{1}$$

Equation (1) denotes the standard normal cumulative distribution function $\Phi(\cdot)$, S_D as the demand median in terms of an IM, and $\beta_{D|IM}$ as the lognormal standard deviation. A linear power law model is usually used to approximate the relationship between median demand and IM which is given in Eq. (2) as below:

$$S_D = a(IM)^b \tag{2}$$

If the results plotted on a logarithmic scale, the parameters can be obtained from a linear regression analysis, because in the logarithmic scale, scatter data points are usually linear trend (Fig. 4).

$$\ln(S_D) = \ln(a) + b \cdot \ln(IM) \tag{3}$$

where $\ln(a)$ and b are the linear regression coefficients, which means the vertical intercept and the slope, respectively.

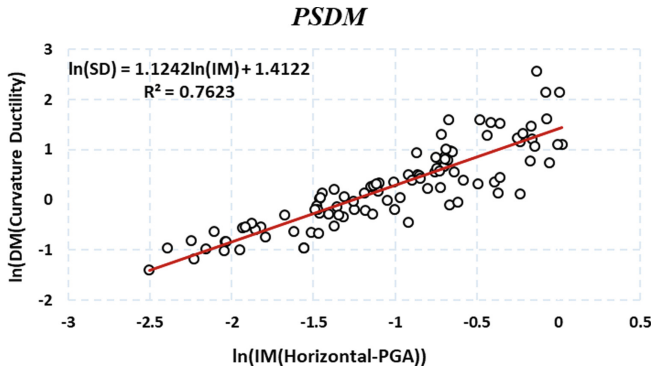


Fig. 5. Probabilistic seismic demand model for curvature EDP and applying two component of earthquake.

One of the PSDMs, which is developed with the curvature ductility engineering demand parameter has been illustrated in Fig. 5.

For estimating the component fragility, a closed-form solution described in Eq. (4) can be used. Where in, D and C represent demand and capacity, respectively.

$$P[D > C|IM] = \Phi \left(\frac{\ln(S_D) - \ln(S_C)}{\sqrt{\beta_{D|IM}^2 + \beta_C^2}} \right) \tag{4}$$

where S_D and S_C denote the median of demand and capacity and $\beta_{D|IM}$ and β_C denote the dispersions of demand and capacity, respectively. In order to define S_C and β_C the limit states, which are specified in the next section must be considered.

3.1 Damage Limit States

The vulnerability of bridge components has been investigated in previous studies, and different indices have been presented to assess their seismic vulnerability [26–28]. In this work, fragility curves for concrete piers were developed based on damage states described in the HAZUS-MH code [29], which include slight, moderate, extensive, and complete damages. Quantifying these states requires defining the numerical limitation of these states. This study utilized the values provided by Desroches et al. [18] in order to determine the performance level of the bridge pier for the curvature ductility index. However, four limitation states, which cover the damage level, were described for the strain index based on the steel and concrete material in the RC pier. Table 1 illustrates that the slight damage state (DS-1) describes a cracked concrete cover, with the first reinforcement yielding. The moderate damage state (DS-2) consists of spall damage to the cover’s concrete and reaching it to the ultimate compressive strain in addition to

yielding longitudinal reinforcements. In the extensive damage state (DS-3), the cover concrete is completely collapsed, and the strain of that exceeds the failure strain. In this state, the longitudinal reinforcement may or may not be buckled. The complete damage state (DS-4) describes the core’s concrete crushing and buckling reinforcement. In this regard, the first moment at which the confined concrete reaches or exceeds its ultimate compressive strain is taken into account.

Table 1. Description of strain damage limit states.

Damage State	Damage Description	Concrete Strain Limits	Reinforcements Strain Limits
DS-1:Slight	Cracking of cover concrete	$\epsilon_{ctu} \leq \epsilon_{ccover} \leq \epsilon_{cunconfined}$	$\epsilon_{sy} \leq \epsilon_s < \epsilon_{bb}$
DS-2:Moderate	Spalling of cover concrete	$\epsilon_{ccover} \geq \epsilon_{cunconfined}$	$\epsilon_{sy} \leq \epsilon_s < \epsilon_{bb}$
DS-3:Extensive	Failure of Cover Concrete	$\epsilon_{ccover} \geq \epsilon_{cfailure}$	$\epsilon_{sy} \leq \epsilon_s \leq \epsilon_{bb}$
DS-4:Complete	Crushing of core concrete and bar buckling	$\epsilon_{ccore} \geq \epsilon_{cconfined}$	$\epsilon_s \geq \epsilon_{bb}$

4 Comparison of Results

4.1 Forces Demands

In this study, the demands of the minimum compressive axial load, maximum compressive axial load, shear load, and bending moment of the RC pier were assessed and compared with and without applying the vertical component of the earthquake. Figure 6 illustrates the changing trend of the minimum compressive axial load. The vertical axis illustrates the value of the compressive axial load demand along the column by applying the vertical component of the earthquake, while the horizontal axis illustrates the earthquake records applied to the bridge model, which are numbered from 1 to 100. Based on the diagram, applying the vertical component of the earthquake reduces the minimum compressive load, resulting in some records showing a zero value for this load. The zero value for the minimum compressive load along the column means the load direction has changed from compression to tensile all over the RC pier.

Figure 7 compares the maximum compressive force in the pier in two different states of analysis. In this diagram, the vertical axis represents the maximum compressive force of the RC column, normalized to its pure compressive force capacity (P_c). According to the diagram, the demand for the bridge structure has increased in most records that apply the vertical component of an earthquake to the bridge structure. At its maximum state, this increase only affects around 25% of the column’s pure compressive force.

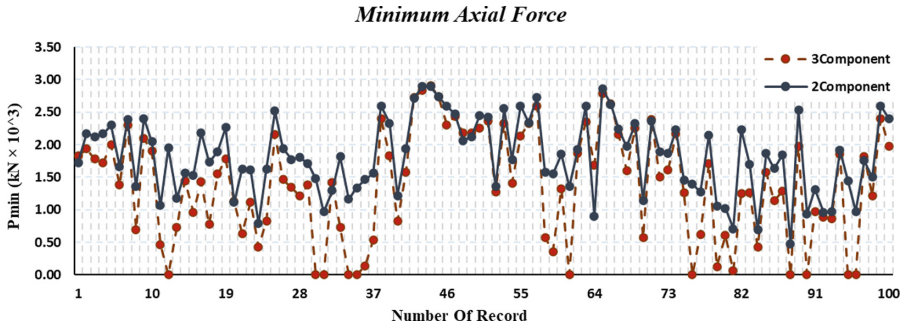


Fig. 6. Minimum compressive axial load with and without considering the vertical component of the earthquake.

Additionally, the impact of the vertical component of the earthquake on the shear force and bending moment of the pier was investigated. According to the results, the vertical component of the earthquake increased them. The value of this increase was 7% in the shear force and 9% in the bending moment.

The bar graphs are developed in Fig. 8 to compare the data average for four obtained demand values from the nonlinear time history analysis of all 100 records in order to simplify the comparison of the parameters mentioned.

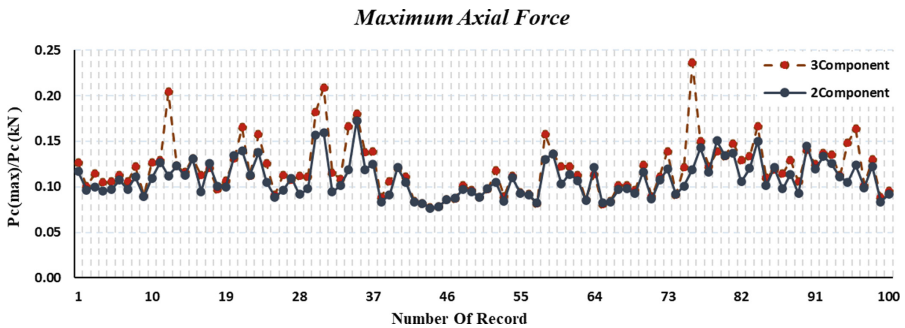


Fig. 7. Maximum compressive axial load with and without considering the vertical component of the earthquake.

4.2 Fragility Analysis

Based on Sect. 3.1 and the specified damage states, fragility curves were developed based on Fig. 9 using two indices including curvature ductility and strain. A dynamic nonlinear time history analysis was performed with and without considering the vertical component of the earthquake in order to extract the outputs of each damage state and compare the fragility curves in both scenarios.

Figure 9(a) shows the bridge vulnerability in four damage states with the curvature ductility index. It can be seen in the figure that the vertical component of the earthquake

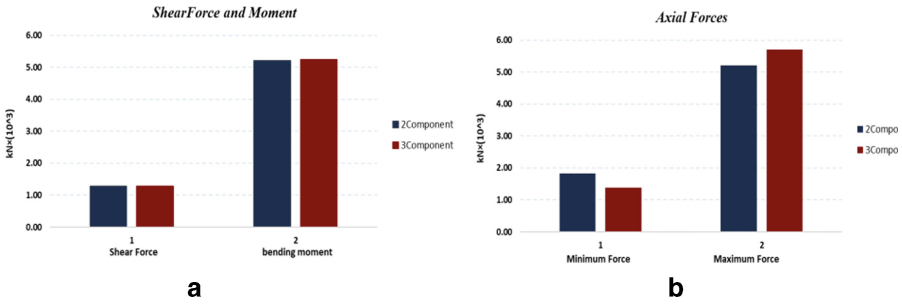


Fig. 8. Average of demand for (a) Axial forces and (b) Shear force and bending moment.

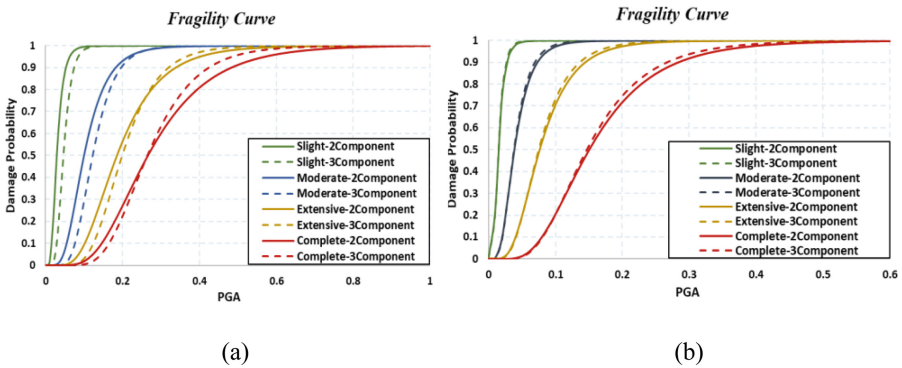


Fig. 9. Fragility curves (a) Curvature damage index and (b) Strain damage index.

had no effect on the vulnerability increase in moderate and slight states, and the results indicate a reduction in vulnerability in these states. In higher damage states, however, the vulnerability increased after the 0.25 g acceleration. Figure 9(b) studied the vulnerability of the bridge using the RC pier strain index based on the specified states. As a consequence, an increase in the damage possibility was observed in all states after applying the vertical component of the earthquake. The increase is greater in the higher damage states.

Accordingly, in Fig. 10 fragility curves for four damage states were presented separately for two indices of strain and curvature ductility in order to scrutinize the investigation of both indices. It is evident that in a similar IM, the strain index shows a higher damage percentage compared to the curvature ductility index.

Using the earthquake strain index, the probability of a moderate damage state at 0.1 g acceleration and applying two components of the earthquake is about 95%, whereas the curvature ductility index makes the possibility of this damage state 50%. Therefore, the strain index indicates that the 0.1 g acceleration will cause a spall in the concrete of the cover, and the curvature ductility index reduces the probability to 50%. By applying the vertical component of the earthquake, the curvature ductility index shows a reduction in failure probability, while the strain index indicates an increase. Similarly, the result

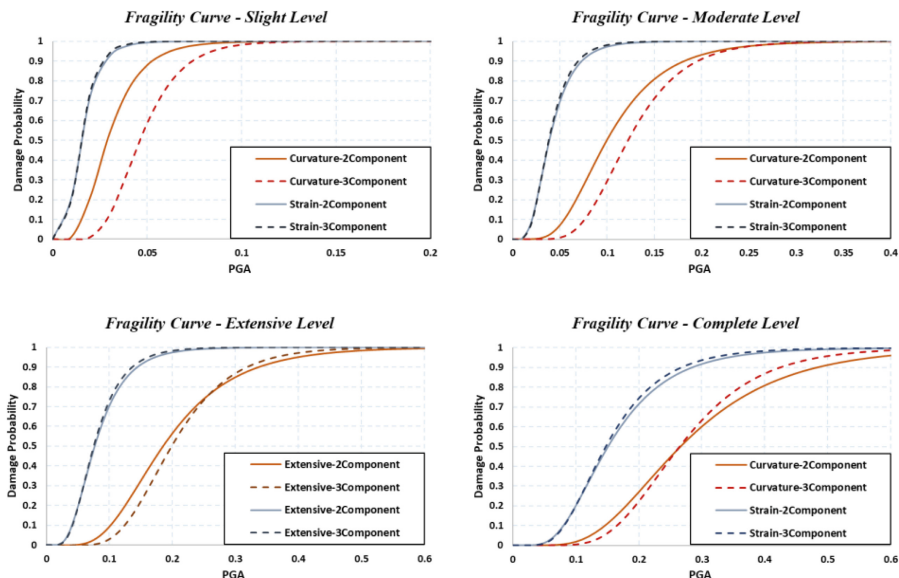


Fig. 10. Four damage level fragility curves with strain and curvature ductility indices.

analysis in other damage states verified the higher accuracy of the strain index in showing damage whether two or three components are applied.

5 Summary and Conclusion

In this paper, two damage indices including strain and curvature ductility have been used to develop the fragility curves of RC bridge columns with PSDM under a series of ground motion records. The variation of axial force, bending moment, and shear force have been investigated and the following results were obtained:

1. The results show that applying the vertical component of the earthquake increases the maximum compressive axial load, shear force, and bending moment in the RC bridge pier and reduces the minimum compressive force.
2. In all four damage states, the damage possibility increased by applying the vertical component of the earthquake with respect to the strain damage index, but according to the curvature ductility index, it increased only in higher damage states (complete-extensive) and after acceleration of 0.25g.
3. The results show that in a specified IM, the strain index shows a higher damage percentage than the curvature ductility damage index.

References

1. California Department of Transportation (Caltrans). Caltrans seismic design criteria, version 1.7 (2013)
2. Papazoglou, A.J.: Near-source vertical earthquake ground motion; An assessment of causes and effects. Imperial College (1995)
3. Elnashai, A.S., Papazoglou, A.J.: Vertical earthquake ground motion: Evidence, effects and simplified analysis procedures. Civil Engineering Department, Imperial College (1995)
4. Haji-Soltani, A., Pezeshk, S., Malekmohammadi, M., Zandieh, A.: A study of vertical-to-horizontal ratio of earthquake components in the golf coast region. *Bull. Seismol. Soc. Am.* **107**(5), 2055–2066 (2017)
5. Hall, J.F. (ed.): Northridge earthquake reconnaissance report. *Earthquake Spectra*, Supplement C to Volume 11, April (1995)
6. Broderick, B.M., Elnashai, A.S., Ambraseys, N.N., Barr, J.M., Goodfellow, R.G., Higazy, E.M.: The Northridge (California) earthquake of 17 January 1994: Observations, strong motion and correlative response analyses. In: *Engineering Seismology and Earthquake Engineering*, Research Report No. ESEE, vol. 94, no. 4 (1994)
7. Goltz, J.D.: The Northridge, California earthquake of January 17, 1994: General reconnaissance report. In: *The Northridge, California Earthquake of January 17, 1994: General Reconnaissance Report*, p. 202 (1994)
8. Rasouli, M., Shiravand, M.R., Rasti Ardakani, R: Performance-based design method for isolated hollow RC piers with irregularity in height. *Struct. Concr.* (2022)
9. Saadeghvariri, M.A., Foutch, D.A.: Dynamic behavior of R/C highway bridges under the combined effect of vertical and horizontal earthquake motions. *Earthq. Eng. Struct. Dyn.* **20**, 535–549 (1991)
10. Saadeghvaziri, M.A., Foutch, D.A.: Inelastic response of R/C highway bridges under the combined effect of vertical and horizontal earthquake motions. *Struct. Res. Ser.* **540** (1998)
11. Papazoglou, A.J., Elnashai, A.S.: Analytical and field evidence of the damaging effect of vertical earthquake ground motion. *Earthq. Eng. Struct. Dyn.* **25**(10), 1109–1137 (1996)
12. Broderick, B.M., Elnashai, A.S.: Analysis of the failure of Interstate 10 freeway ramp during the Northridge earthquake of 17 January 1994. *Earthq. Eng. Struct. Dyn.* **24**(2), 189–208 (1995)
13. Yu, C.P.: Effect of vertical earthquake components on bridge responses. The University of Texas at Austin (1996)
14. Yu, C.P., Broekhuizen, D.S., Roesset, J.M.: Effect of vertical ground motion on bridge deck response. In: *Post-Earthquake Reconstruction Strategies: NCEER-INCEDE Center-to-Center Project*, pp. 249–263 (1997)
15. Button, M.R., Cronin, C.J., Mayes, R.L.: Effect of vertical motions on seismic response of highway bridges. *J. Struct. Eng.* **128**(12), 1551–1564 (2002)
16. Abdelkareem, K.H., Machida, A.: Effects of vertical motion of earthquake on failure mode and ductility of RC bridge piers. In: *Proceedings of the 12th World Conference on Earthquake Engineering*, Auckland, New Zealand, Paper (No. 0463) (2000)
17. Kunnath, S.K., Erduran, E., Chai, Y.H., Yashinsky, M.: Effect of near-fault vertical ground motions on seismic response of highway overcrossings. *J. Bridg. Eng.* **13**(3), 282–290 (2008)
18. DesRoches, R., Padgett, J., Ramanathan, K., Dukes, J.: Feasibility studies for improving Caltrans bridge fragility relationships (No. CA12-1775) (2012)
19. Rassoulpour, S., Shiravand, M.R., Safi, M.: Proposed seismic-resistant dual system for continuous-span concrete bridges using self-centering cores. *Eng. Struct.* **274**, 115181 (2023)
20. OpenSees. Open System for Earthquake Engineering Simulation, Pacific Earthquake Engineering Research Center, University of California, Berkeley, (2006). <http://opensees.berkeley.edu/>

21. Mander, J.B., Priestley, M.J., Park, R.: Theoretical stress-strain model for confined concrete. *J. Struct. Eng.* **114**(8), 1804–1826 (1988)
22. Menegotto, M., Pinto, P.E.: Method of analysis for cyclically loaded reinforced concrete plane force and bending. In: *Proceedings, IABSE Symposium on Resistance and Ultimate Deformability of Structures Acted on by Well Defined Repeated Loads*, Lisbon, 15–22 (1973)
23. Baker, J.W.: *Vector-Valued Ground Motion Intensity Measures for Probabilistic Seismic Demand Analysis*. Stanford University (2005)
24. Padgett, J.E., Nielson, B.G., DesRoches, R.: Selection of optimal intensity measures in probabilistic seismic demand models of highway bridge portfolios. *Earthq. Eng. Struct. Dyn.* **37**(5), 711–725 (2008)
25. Cornell, C.A., Jalayer, F., Hamburger, R.O., Foutch, D.A.: Probabilistic basis for 2000 SAC federal emergency management agency steel moment frame guidelines. *J. Struct. Eng.* **128**(4), 526–533 (2002)
26. Mahboubi, S., Shiravand, M.R.: Proposed input energy-based dam-age index for RC bridge piers. *J. Bridg. Eng.* **24**(1), 04018103 (2019). [https://doi.org/10.1061/\(ASCE\)BE.1943-5592.0001326](https://doi.org/10.1061/(ASCE)BE.1943-5592.0001326)
27. Mahboubi, S., Shiravand, M.R.: Seismic evaluation of bridge bearings based on damage index. *Bull. Earthq. Eng.* **17**(7), 4269–4297 (2019)
28. Mahboubi, S., Kioumars, M.: Damage assessment of RC bridges considering joint impact of corrosion and seismic loads: A systematic literature review. *Constr. Build. Mater.* (2021). <https://doi.org/10.1016/j.conbuildmat.2021.123662>
29. HAZUS. Earthquake model. HAZUS-MH 2.0: Technical Manual. Federal Emergency Management Agency, Washington DC (2009)